Drug Design, Development and Therapy

Dovepress
Taylor & Francis Group

Open Access Full Text Article

ORIGINAL RESEARCH

Astragaloside IV Promotes Osteogenic Differentiation of Periodontal Ligament Stem Cells via Activating PI3K/AKT/eNOS/NO Signaling Pathway: In vitro and in vivo Study

Yang Song[1–3], Jing Hu[1–3], Peng Yang[1–3], Yuxing Zhang[1–3], Zhaoyan Wu[1–3], Siyu Chen[1–3], Jun Zhang[1–3]

[1]Department of Orthodontics, School and Hospital of Stomatology, Cheeloo College of Medicine, Shandong University, Jinan, People's Republic of China; [2]Shandong Key Laboratory of Oral Tissue Regeneration, Jinan, People's Republic of China; [3]Shandong Engineering Research Center of Dental Materials and Oral Tissue Regeneration, Jinan, People's Republic of China

Correspondence: Jun Zhang, Department of Orthodontics, School and Hospital of Stomatology, Cheeloo College of Medicine, Shandong University, No. 44-1 Wenhua Road West, Jinan, Shandong, 250012, People's Republic of China, Tel +86 13953109816, Fax +86 53188382923, Email zhangj@sdu.edu.cn

Purpose: Periodontal ligament stem cells (PDLSCs) play a critical role in alveolar bone regeneration and orthodontics. Astragaloside IV (AS-IV) is the chief ingredient of Astragalus, which has been shown to promote osteogenesis. The study aimed to detect the impact of AS-IV on osteogenic differentiation of PDLSCs and to investigate the role of the PI3K/AKT/eNOS/NO pathway in this process.

Methods: PDLSCs were isolated from clinically healthy premolars that were extracted for orthodontic purposes from patients aged 14–20 years. The isolated cells were then cultured in vitro and characterized by flow cytometry. After treating the cells with different doses of AS-IV, LY294002 (PI3K inhibitor), and L-NAME (eNOS inhibitor), alkaline phosphatase (ALP) staining, alizarin red staining, qRT-PCR, Western blotting, nitric oxide (NO) assay and immunofluorescence staining were utilized to ascertain the expression level of related factors and the validity of PI3K/AKT/eNOS/NO pathway. Divided sixteen male Wistar rats into the control and AS-IV groups, and the orthodontic tooth movement model was created for 14 days. Micro-computed tomography scan, hematoxylin and eosin staining and immunohistochemical staining were conducted to investigate relevant indicators.

Results: PDLSCs expressed high levels of surface antigens CD44 and CD90 while negatively expressing CD34 and CD45. AS-IV at each experimental concentration did not inhibit the proliferation of hPDLSCs, and 20 μM AS-IV could significantly enhance ALP activity, mineral deposition, and ALP, runt-related transcription factor 2 (RUNX-2), collagen I (COL-1) expression. After adding inhibitors LY294002 and L-NAME, the effect of AS-IV was inhibited. In vivo, AS-IV increased bone volume/total volume (BV/TV), trabecular thickness (Tb. Th), and the expression of ALP, COL-1 and eNOS on the tension side in rats.

Conclusion: AS-IV can promote the osteogenic differentiation of PDLSCs, and PI3K/AKT/eNOS/NO was involved. Meanwhile, AS-IV exhibits positive effects on tension-side osteogenesis during tooth movement in rats.

Keywords: Astragaloside IV, periodontal ligament stem cells, osteogenic differentiation, PI3K/AKT/eNOS/NO

Introduction

Healthy periodontal tissue is fundamental to maintaining proper occlusion function. The regulation of periodontal tissue remodeling and regeneration has always been a significant concern in dentistry, with alveolar bone reconstruction being one of its most critical aspects. As the emphasis on oral and maxillofacial aesthetics increases, more people are undergoing orthodontic treatment, resulting in orthodontic tooth movement (OTM) and relapse becoming common clinical scenarios involving dynamic periodontal tissue remodeling. Both of them have similar tissue structure and response, with periodontal tissue undergoing bone formation on tension side and bone resorption on pressure side.[1] How to better promote periodontal osteogenesis is a topic deserving in-depth study, which is clinically essential for orthodontic

Received: 28 December 2024
Accepted: 7 July 2025
Published: 16 July 2025

tooth movement and recurrence process regulation, orthodontic anchorage control, and reconstruction of periodontal tissue defects. Periodontal ligament stem cells (PDLSCs) have strong clonal proliferation ability and can differentiate into periodontal tissues including alveolar bone,[2,3] which plays a vital role in tissue reconstruction and regeneration engineering.[4–6] Various exogenous and endogenous factors can affect the proliferation and differentiation of PDLSCs, including growth factors (eg, fibroblast growth factor-2), dietary supplements (eg, rutin, naringin), drugs (eg, metformin, strontium), mechanical forces, etc.[6,7]

Astragalus membranaceus is useful as a tonic for treating osteoporosis.[8] Astragaloside IV (AS-IV), one of the chief active ingredients of *Astragalus membranaceus*, is a tetracyclic triterpenoid saponin in the form of lanosterol.[9] Many studies have found that AS-IV has a variety of activities as anti-inflammatory, antioxidant, antifibrotic, antiviral, etc., and exerts functions such as osteogenesis, angiogenesis promotion and vasodilation, inhibition of neuronal apoptosis, etc.[10–16] Phosphatidylinositol 3 kinase/protein kinase B (PI3K/AKT) pathway exists in a wide range of biological phenomena including bone metabolism. It can facilitate the proliferation and differentiation of osteoblasts under excitation of certain substances.[17,18] Nitric oxide (NO) is a vital signaling agent that regulates various functions in stem cells, and the physiological amount of NO is indispensable for the maintenance of PDLSCs osteogenic differentiation.[19–21] Endogenous NO is mainly induced by nitric oxide synthase (NOS), which has three isoforms: endothelial NOS (eNOS), inducible NOS (iNOS), and neuronal NOS (nNOS), and it has been proven that PDLSCs significantly expressed eNOS and iNOS but lowly expressed nNOS.[22,23] Defective NOS will lead to defective osteogenesis,[24–26] and tension-side cells significantly express eNOS during orthodontic tooth movement.[27,28]

There is evidence that AKT can activate eNOS,[29–31] which has also been proven in the osteogenic processes of osteoblasts.[32–34] However, there is currently a lack of experiments that verify the involvement of the PI3K/AKT/eNOS/NO pathway in the osteogenic differentiation of human PDLSCs. AS-IV can stimulate PI3K/AKT/eNOS/NO pathway to exert anti-inflammatory, pro-vasodilatory, and trauma recovery effects on other cells.[15,35–37] Despite this, its specific influence on the osteogenic differentiation of PDLSCs and the underlying mechanisms remain unclear. Therefore, we hypothesized that AS-IV might similarly encourage the osteogenic differentiation of PDLSCs through the same pathway, and designed relevant experiments to serve as a valuable reference for the future clinical application.

Materials and Methods

Cell Culture and Identification

This assay was carried out after obtaining the clearance of Ethical Committee of Shandong University School of Stomatology (No. 20221004). With permission from the legal guardians, complete and caries-free premolars removed for orthodontic need were collected from patients aged 14 to 20 years. Minimum essential medium (MEM, Basalmedia, Shanghai, China) containing 5% penicillin/streptomycin (Biosharp, Beijing, China) was prepared and precooled in advance. The extracted teeth were promptly kept in the centrifuge tube with the medium, and the root surface was gently washed by phosphate buffered saline (PBS, Basalmedia, Shanghai, China) to remove the attached blood. In an ultra-clean workstation, collected the periodontal ligament from the root within four hours after the tooth extraction. The pieces were tiled in the culture flask and added with 5 mL MEM, including 1% antibiotics and 20% fetal bovine serum (FBS, Yeasen, Shanghai, China). About 4 hours later, when the pieces were attached successfully, the flask was turned over and placed in the incubator at 37°C with 5% CO_2. Once the PDLSCs protruded from the edge of the tissue pieces and reached 80% confluence, they were digested with 0.25% trypsin-EDTA solution (Biosharp, Beijing, China) in the incubator, then terminated the process 1 minute later by adding MEM supplemented with 10% FBS. Centrifuged, resuspended, and placed the cells in culture dishes at a ratio of 1:2 or 1:3. The following experiments were conducted using the PDLSCs at passages 3–5. To determine the stem cell characteristics of the cultivated PDLSCs, cell surface markers consisting of CD34, CD44, CD45, and CD105 were identified by flow cytometer.

Multidirectional Differentiation Assays

Cells were seeded in 6-well plates at a density of 1×10^5 cells per well and incubated with osteogenic induction medium (MEM with 10% FBS, 50μg/mL ascorbic acid, 0.01μM dexamethasone, and 10mM β-glycerophosphate, Solarbio,

Beijing, China) or adipogenic induction medium (MEM with 10% FBS, 500mM isobutyl-methylxanthine, 10 mM insulin, 60mM indomethacin, and 0.5 M hydrocortisone, Solarbio, Beijing, China). The medium was removed after 28 days of culture. Cells were fixed by 95% ethanol or 4% paraformaldehyde at room temperature. After rinsing three times, the cells were stained with Alizarin Red S or Oil Red O (Beyotime, Shanghai, China). The mineralized nodules and lipid droplets were captured by microscope.

Cell Proliferation Assay

The influence of AS-IV on PDLSCs proliferation was tested by cell counting kit-8 (CCK-8, Biosharp, Beijing, China) to assist in determining the optimal concentration. In this assay, PDLSCs were routinely digested, resuspended, and seeded in 96-well plates at a density of 3×10^3 cells per well. 24 hours later, the solution was changed to the complete medium containing AS-IV (MedChemExpress, New Jersey, USA) at concentrations of 0, 0.1, 1, 10, 20, and 40 μM. After 2-hour incubation at 37°C in the dark, the culture medium was substituted for 100μL of CCK-8 working reagent on day 1, 3, and 5. Absorbance values were examined at 450 nm.

Alizarin Red Staining and Alkaline Phosphatase (ALP) Activity Assay

According to the experimental requirements, PDLSCs were cultured in the osteogenic inducing medium containing 0, 0.1, 1, 10, 20, and 40 μM AS-IV. After 28 days, PDLSCs were fixed with 95% ethanol and subsequently stained with Alizarin Red S to evaluate the mineralized nodules by observing and photographing under a light microscope. Additionally, 10% cetylpyridinium chloride was utilized in order to quantify the amount of mineralized matrix deposition. Absorbance of the solution was assayed at 562 nm.

Cells were cultivated as previously described. After 14 days of incubation, cells were solubilized in the lysate solution (RIPA: PMSF=99:1) (Solarbio, Beijing, China) and scraped off after 30 minutes on ice. The gathered solution was ultrasonically lysed and centrifuged at 4°C to extract the supernatant-obtaining protein. ALP activity was tested by alkaline phosphatase assay kit (Jiancheng, Nanjing, China), while protein concentration was tested by bicinchoninic acid kits (Yeasen, Shanghai, China). Visualized ALP staining by the BCIP/NBT alkaline phosphatase color development kit (Beyotime, Shanghai, China) and captured the images with a scanner.

Quantitative Real-Time Reverse Transcriptase-Polymerase Chain Reaction (qRT-PCR)

Following 14-day osteogenic induction with different concentrations of AS-IV (0, 0.1, 1, 10, 20, and 40 μM), total cellular RNA was extracted using the Trizol method.[38] RNA concentration and purity were determined using a NanoDrop 2000 spectrophotometer, with acceptable A260/A280 ratios between 1.8–2.0. Samples showing abnormal spectrophotometry profiles were excluded. Subsequently, strict RNase-free techniques were maintained throughout all procedures with immediate complementary DNA conversion after extraction. In accordance with the manufacturer's protocol, qRT-PCR was conducted using Hieff® qPCR SYBR Green Master Mix (Yeasen, Shanghai, China), and every reaction system included 3 replicate wells. qRT-PCR was performed with the following cycling parameters: initial denaturation at 95°C for 300 sec, followed by 40 cycles of 95°C for 10 sec and 60°C for 30 sec.

Primer sequences for *ALP, RUNX-2, COL-1*, and *GAPDH* were listed as following: *ALP* (5′-GGCGGTGAACG AGAGAGAATGT-3′ and 5′-GGACGTAGTTCTGCTCGTGG-3′); *RUNX-2* (5′-GCGCATTCCTCATCCCAGTA-3′ and 5′-CCTGCCTGGGGTCTGTAATC-3′); *COL-1* (5′-TAAAGGGGTCACCGTGGGCTTC-3′ and 5′-GGGAGAC CGTTGAGTCCATC-3′); *GAPDH* (5′-ACTCCCATTCTTCCACCTTT-3′ and 5′-CCCTGTTGCTGTAGCCATATT-3′). The $2^{-\Delta\Delta Ct}$ method was applied to quantify the relative mRNA levels, normalizing to *GAPDH* level. Each experiment was repeated five times.

Western Blot

Cells were cultivated with osteogenic induction for 14 days. Extracted protein and detected the concentration as above method, and then separated the protein samples with different molecular weights via 10% SDS-PAGE. After electrophoresis, transferred proteins to a 0.45 μm polyvinylidene fluoride membrane, which was subsequently blocked by the blocking buffer to minimize nonspecific binding. Incubate the membrane with primary antibodies toward target proteins

including ALP (Proteintech, 11187-1-AP, 1:1000), RUNX-2 (ImmunoWay, YM8347, 1:2000), COL-1 (Proteintech, 67288-1-Ig, 1:5000), eNOS (Abways, AB3537, 1:500), iNOS (Abways, CY3425, 1:500), p-AKT (Abways, CY6569, 1:1000), AKT (Abways, CY5561, 1:1000) and GAPDH (Proteintech, 10494-1-AP, 1:5000) overnight at 4°C. After 30-minute washing by TBST solution, the membrane was treated with secondary antibodies (HRP-conjugated Goat Anti-Rabbit IgG (H+L): Proteintech, SA-00001-2, 1:10000; HRP-conjugated Goat Anti-Mouse IgG (H+L): Proteintech, SA-00001-1, 1:10,000). The enhanced chemical hypersensitive luminescent liquid kit (Yeasen, Shanghai, China) and chemical imaging system detected the protein bands. Each experiment was repeated five times.

Immunofluorescence Staining

Cells were washed three times with PBS solution and then immobilized by 4% paraformaldehyde for 20 minutes. After washing the cells again with PBS, 5% bovine serum albumin (BSA) was used to block for 1 hour. Cells were incubated with primary antibodies at 4°C overnight. On the next day, cells were incubated with secondary antibody for 1 hour, and further stained with 2-(4-amidinophenyl)-6-indolecarbamidine dihydrochloride (DAPI) for 5 min in the dark at room temperature. The images were acquired by fluorescence microscope and processed with ImageJ.

NO Concentration Detection

Culture supernatant was gathered and measured using the Griess kit (Beyotime, Shanghai, China), and absorbance value was examined at 540 nm using an enzyme meter. NO_2^- concentration calculated by a standard curve represented the level of NO production.

LY294002 and L-NAME Treatments

LY294002 (MedChemExpress, New Jersey, USA) is a classical broad-spectrum inhibitor of PI3K that inhibits the PI3K/AKT pathway. Divided the cells into four groups: (1) control group with only osteogenic induction solution; (2) osteogenic induction solution + 20 μM AS-IV group; (3) osteogenic induction solution + 10 μM LY294002 group; (4) osteogenic induction medium + 20 μM AS-IV + 10 μM LY294002 group.

Nω-Nitro-L-arginine methyl ester hydrochloride (L-NAME, Beyotime, Shanghai, China) is an eNOS inhibitor. Divided the cells into four groups: (1) control group with only osteogenic induction solution; (2) osteogenic induction solution + 20 μM AS-IV group; (3) osteogenic induction solution + 100 μM L-NAME group; (4) osteogenic induction medium + 20 μM AS-IV + 100 μM L-NAME group.

Animals and Drugs

All experiments involving the rats adhered to the National Institutes of Health Guidelines for the Care and Use of Laboratory Animals and the experiment was authorized by Shandong University's Institutional Ethics Committee (No. 20220343). The required experimental animal size was determined using the resource equation method,[39] with the detailed methodology provided in Supplementary Data 1. 16 male Wistar rats, aged six weeks, weighing an average of 180±20 g, were purchased from SPF biotechnology company (Beijing, China) and raised in standard plastic cages with 21±1°C ambient temperature and 55±10% relative humidity. The circumstance was specific pathogen-free. Every rat was acclimatized for 1 week. Two groups (n=8) consisting of the control and AS-IV groups were randomly and evenly assigned. The AS-IV group received intraperitoneal injections of AS-IV at a dosage of 40 mg/kg/d,[12] whereas the control group administered the identical volume of physiological saline for 14 days.

OTM Model Establishment

After inducing anesthesia with isoflurane, the 25 mg/kg intraperitoneal injection of pentobarbital sodium was administered to each rat. A nickel-titanium closed-coil spring, which produced 30 g orthodontic force, was bolted to the right maxillary first molar, and the other end was secured to the pre-prepared groove in the two maxillary incisors. Bound and reinforced the two maxillary incisors with light-curing resin to prevent device detachment and strengthen anchorage. In the whole tooth movement process, the appliance's integrity and the rat's general condition were monitored daily. 14 days

later, all rats were fixed by cardiac puncture perfusion with 4% paraformaldehyde under anesthesia. Right maxillary molar and surrounding tissue were separated and immersed in 4% paraformaldehyde for 24 to 48 h at 4°C.

Micro-CT

Utilized a micro-computer tomography (micro-CT) scanner setting 88 μA, 90 kV, and 36 μm scanning layer thickness to scan the specimens and converted the raw image into DICOM format by the systematic self-contained algorithm. The digital information was imported into RadiAntViewer to determine the shortest distance between right maxillary second molar's proximal surface and first molar's distal surface as the OTM distance. Two alveolar bone regions (400 μm long, 200 μm wide, and 800 μm high) were selected as the regions of interest(ROI), which were situated alongside the mesial side of distobuccal root as well as distal side of the mesial root of the first molar. DataViewer was used to correct the axis orientation, and CTAn was used to set ROI and calculate BV/TV, Tb. Th and trabecular separation (Tb.Sp).

Histological and Immunochemical Analysis

After fixation was completed, specimens were rinsed for 2–4 h, placed in 10% ethylenediaminetetraacetic acid, and decalcified for more than 8 weeks until the probes could easily puncture the tissue. Next, specimens were rinsed with running water, dehydrated with graded ethanol, washed with xylene, paraffin-embedded, and cut into continuous sagittal paraffin in sections for succeeding experiments. Hematoxylin-eosin (HE, Servicebio, Wuhan, China) was performed to visualize the morphological changes in the tension-side periodontal tissue of maxillary first molar. Immunohistochemical (IHC) staining was carried out using IHC kit (Servicebio, Wuhan, China). Hydrogen peroxide solution was applied to the sections to reduce non-specific staining caused by endogenous peroxidase. ALP, COL-1 and eNOS antibodies (Servicebio, Wuhan, China) were diluted beforehand and the samples were incubated with diluent. Following three PBS washing, the samples were treated with the biotin-labeled secondary antibody (Servicebio, Wuhan, China). Washed the slices again and processed them with the IHC kit based on the reagent instructions.

Statistical Analysis

To ensure blinding and consistency, the group assignments were kept hidden from the personnel performing the measurements, and the same individual conducted all measurements in five repetitions. All analyses were based on five independent experiments. Given the small sample size per group, bootstrap resampling was applied. The average of the measurements was used as the final result. Data were presented as the mean ± standard deviation (mean ± SD).

Statistical analysis was performed using GraphPad Prism software (version 8, MacKiev Software, Boston, MA, USA). Normality of quantitative datasets was confirmed by Shapiro–Wilk test, and variance homogeneity was verified by *F*-test. Having satisfied these parametric assumptions, data were subsequently analyzed by either one-way or two-way ANOVA, followed by Tukey's test for post hoc analysis. A value of $P < 0.05$ was considered statistically significant.

Results

Isolation, Cultivation and Characterization of PDLSCs

Cells cultured to the 3–5 passages were chosen for subsequent assays (Figure 1A). After osteogenic and adipogenic induction cultures, PDLSCs were stained and showed the capacity of multiple differentiation (Figure 1B and C). The mesenchymal stem cell markers CD44 and CD105 were positively expressed in the flow cytometry assay, whereas the surface markers CD34 and CD45 unique to hematopoietic stem cells were negatively expressed (Figure 1D).

Effect of AS-IV on the Proliferation

On day 1, 3, and 5, the effects of different AS-IV concentrations (0, 0.1, 1, 10, 20, and 40 μM) on PDLSCs proliferation were observed. The data demonstrated that different experimental concentrations of AS-IV had no significant inhibitory effect (Figure 2A).

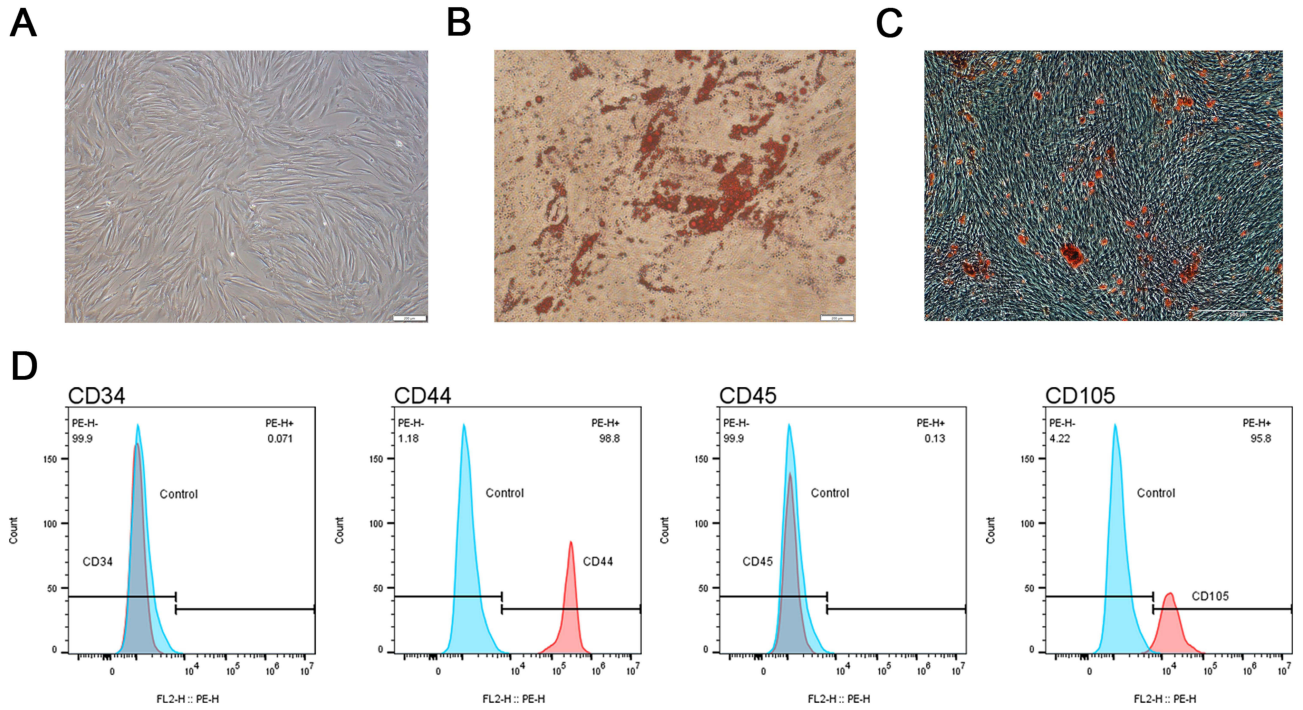

Figure 1 Cultivation and identification of PDLSCs. (**A**) Morphology of PDLSCs. Scale Bar: 200 μm. (**B**) Lipid droplets of PDLSCs after adipogenic induction. Scale bar: 200 μm. (**C**) Mineralized nodules of PDLSCs after osteogenic induction. Scale bar: 500 μm. (**D**) Flow cytometric analyses of PDLSCs. Mesenchymal stem cell markers (CD44, CD105) were positive and hematopoietic stem cell markers (CD34, CD45) were negative in PDLSCs.

Effects of AS-IV on ALP Activity and Mineralized Nodule Formation

ALP activity experiment showed that after 14-day osteogenic induction, all concentrations of AS-IV in the experimental group could promote ALP activity, with the most obvious effect in the 20 μM group (Figure 2B), which matched the trend of ALP staining results (Figure 2D). The mineralized nodule staining and quantitative results also showed that 20 μM AS-IV could significantly increase the formation of mineralized nodules (Figure 2C and E).

AS-IV Promoted the Osteogenesis-Related m-RNA and Proteins

After the 14-day osteogenic induction, ALP, RUNX-2, and COL-1 were detected by qRT-PCR and verified that 20 μM AS-IV had a significant promoting effect (Figure 2F–H). Subsequently, Western blot detection of ALP, RUNX-2, and COL-1 was performed, and the gray value analysis results were statistically different, consistent with the qRT-PCR trend (Figure 2I–L). Combining the above experimental results, we chose 20 μM as the concentration of AS-IV for subsequent experiments.

Osteogenic Promotion of AS-IV Could Be Inhibited by LY294002 and L-NAME

ALP staining experiments showed that LY294002 significantly attenuated the promotion of ALP expression by AS-IV (Figure 3A and D). Immunofluorescence staining revealed LY294002 inhibited the stimulation of COL-1 by AS-IV (Figure 3B and E). Western blot experiments also indicated that AS-IV activated the osteogenic proteins while their expressions were reduced by this inhibitor (Figure 3H–K). To evaluate the optimal time point for activating p-AKT/AKT and NOS after administering AS-IV, we selected 6 time points (0, 5, 10, 15, 30, and 60 minutes) to measure protein expression levels, and we found that p-AKT and eNOS was significantly activated after adding AS-IV for 10min (Figure 3L and O). Western blot showed the expression of p-AKT/AKT was decreased by LY294002 (Figure 3P and S). The above results demonstrated that AS-IV can play an osteogenic role through PI3K/AKT pathway.

Meanwhile, ALP staining (Figure 4A and B), immunofluorescence staining of COL-1 (Figure 4C and D) and Western blot (Figure 4E–J) revealed that L-NAME lowered the expressions of osteogenic-related factors and eNOS, which implies that eNOS is also the critical element enabling AS-IV to exert its osteogenic effects.

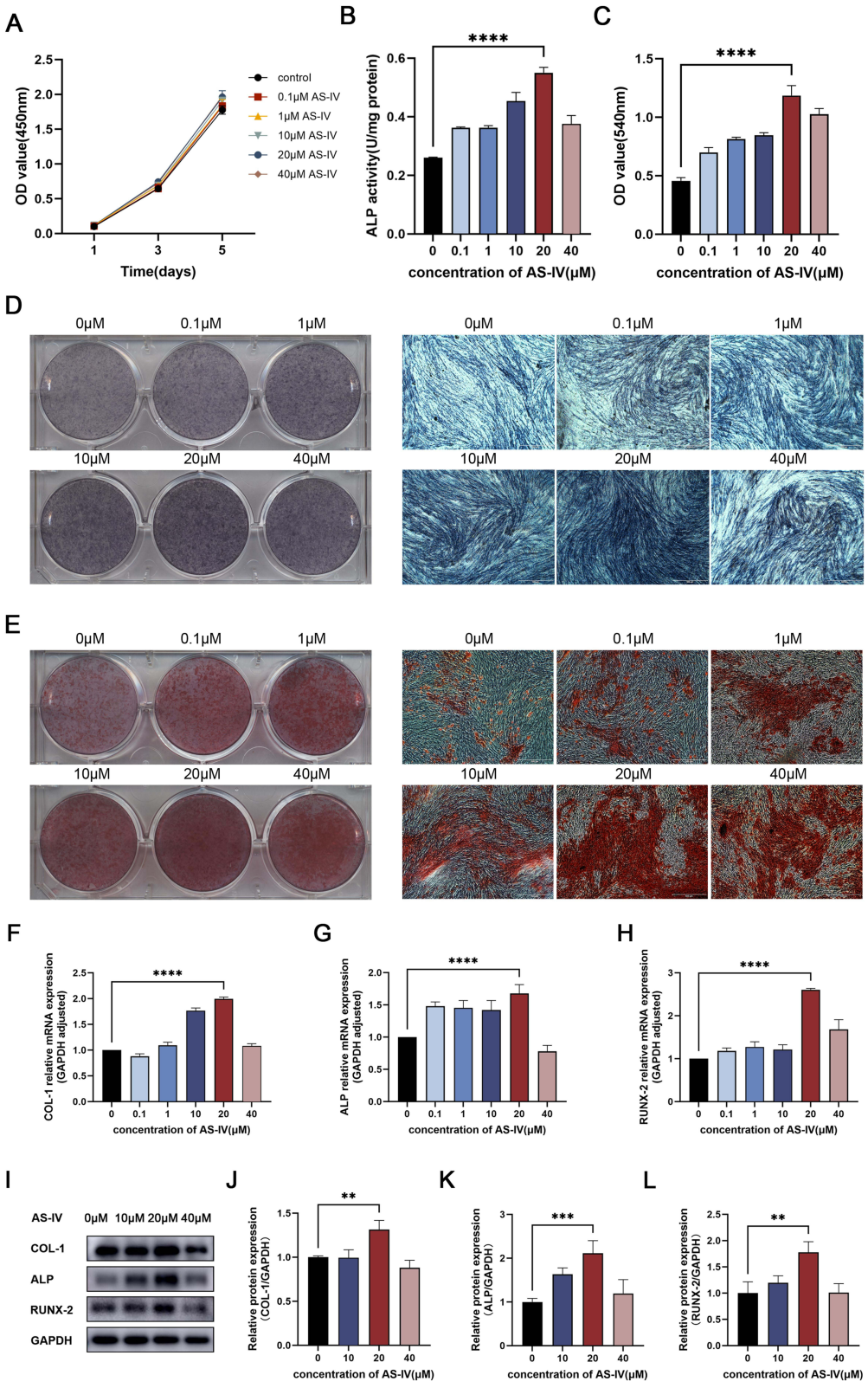

Figure 2 Effect of AS-IV on proliferation and osteogenic differentiation of PDLSCs. (**A**) CCK-8 analysis of AS-IV effects on PDLSCs on day 1, 3, and 5. (**B** and **C**) ALP activity (**B**) and extracellular matrix mineralization (**C**) quantification of PDLSCs affected by AS-IV. (**D**) ALP staining. Scale bar: 500 μm. (**E**) Alizarin Red staining. Scale bar: 500 μm. (**F**–**H**) qRT-PCR analysis of COL-1 (F), ALP(G), and RUNX-2 (**H**) in PDLSCs cultured with AS-IV. (**I**–**L**) Western blot and semi-quantitative analysis of COL-1 (J), ALP(K), and RUNX-2 (**L**) in PDLSCs cultured with AS-IV. 20 μM AS-IV group had a significant promoting effect. Data are presented as mean ± SD. ***P*<0.01, ****P*<0.001, *****P*<0.0001. Each experiment was repeated five times.

https://doi.org/10.2147/DDDT.S514682

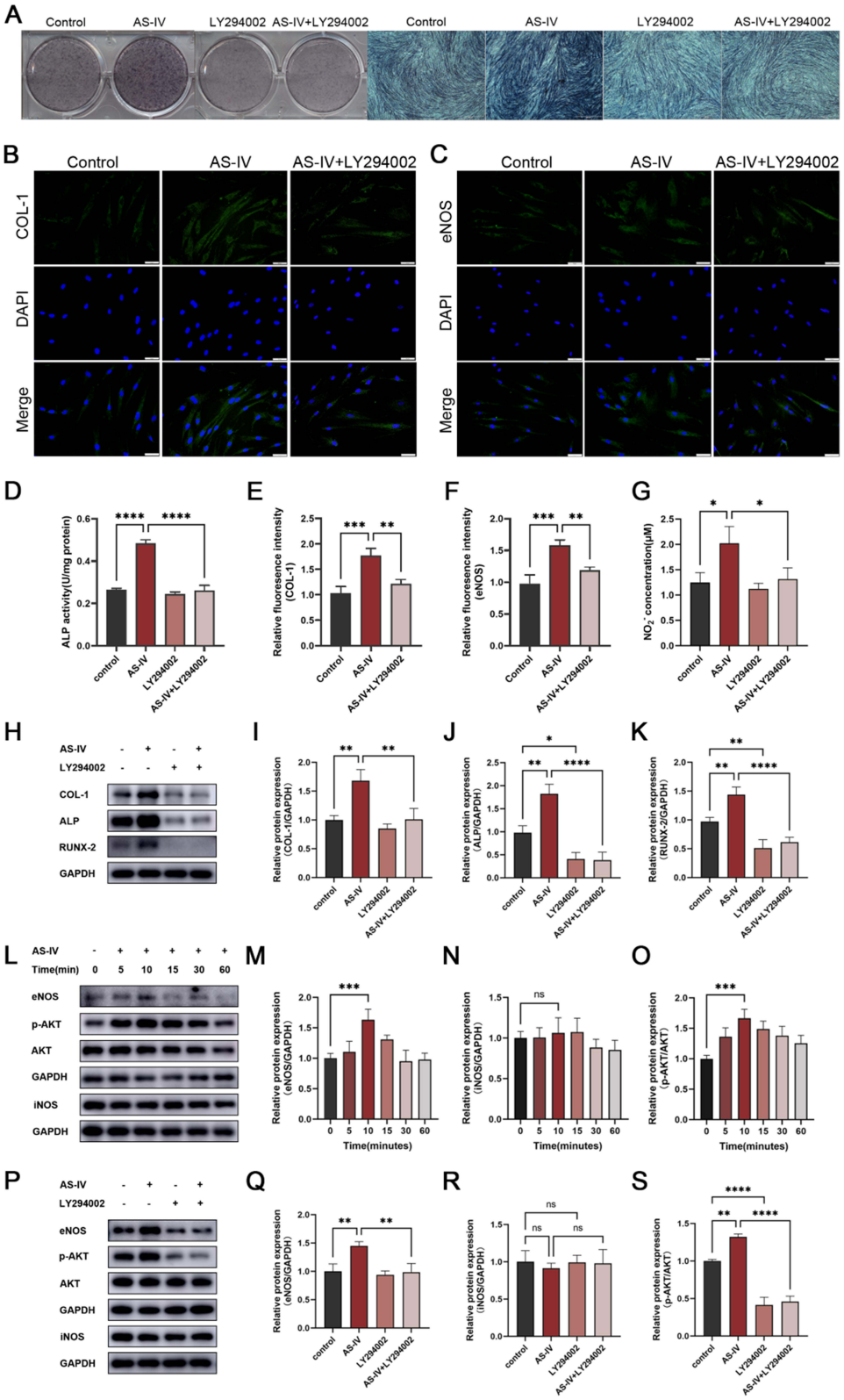

Figure 3 Effect of LY294002 on osteogenic differentiation and pathway-associated factor of PDLSCs following AS-IV incubation. (**A** and **D**) ALP staining(**A**) and ALP activity quantification(**D**) of PDLSCs affected by LY294002. Scale bar: 500 μm. (**B** and **E**) Immunofluorescence staining(**B**) of COL-1 (green) and DAPI staining (blue) and quantification(E). Scale bar: 50 μm. (**C** and **F**) Immunofluorescence staining(**C**) of eNOS (green) and DAPI staining (blue) and quantification(F). Scale bar: 50 μm. (**G**) NO2- concentration represented the level of NO in cell supernatants. (**H–K**) Western blot and semi-quantitative analysis of COL-1(I), ALP(J), and RUNX-2 (**K**) in PDLSCs cultured with AS-IV and LY294002. (**L–O**) Western blot and semi-quantitative analysis of eNOS(M), iNOS(**N**) and p-AKT/AKT (**O**) after addition of AS-IV at different time points. (**P–S**) Western blot and semi-quantitative analysis of eNOS(Q), iNOS(**R**) and p-AKT/AKT (**S**) in PDLSCs cultured with AS-IV and LY294002. Data are presented as mean ± SD. **P*<0.05, ***P*<0.01, ****P*<0.001, *****P*<0.0001. Each experiment was repeated five times.

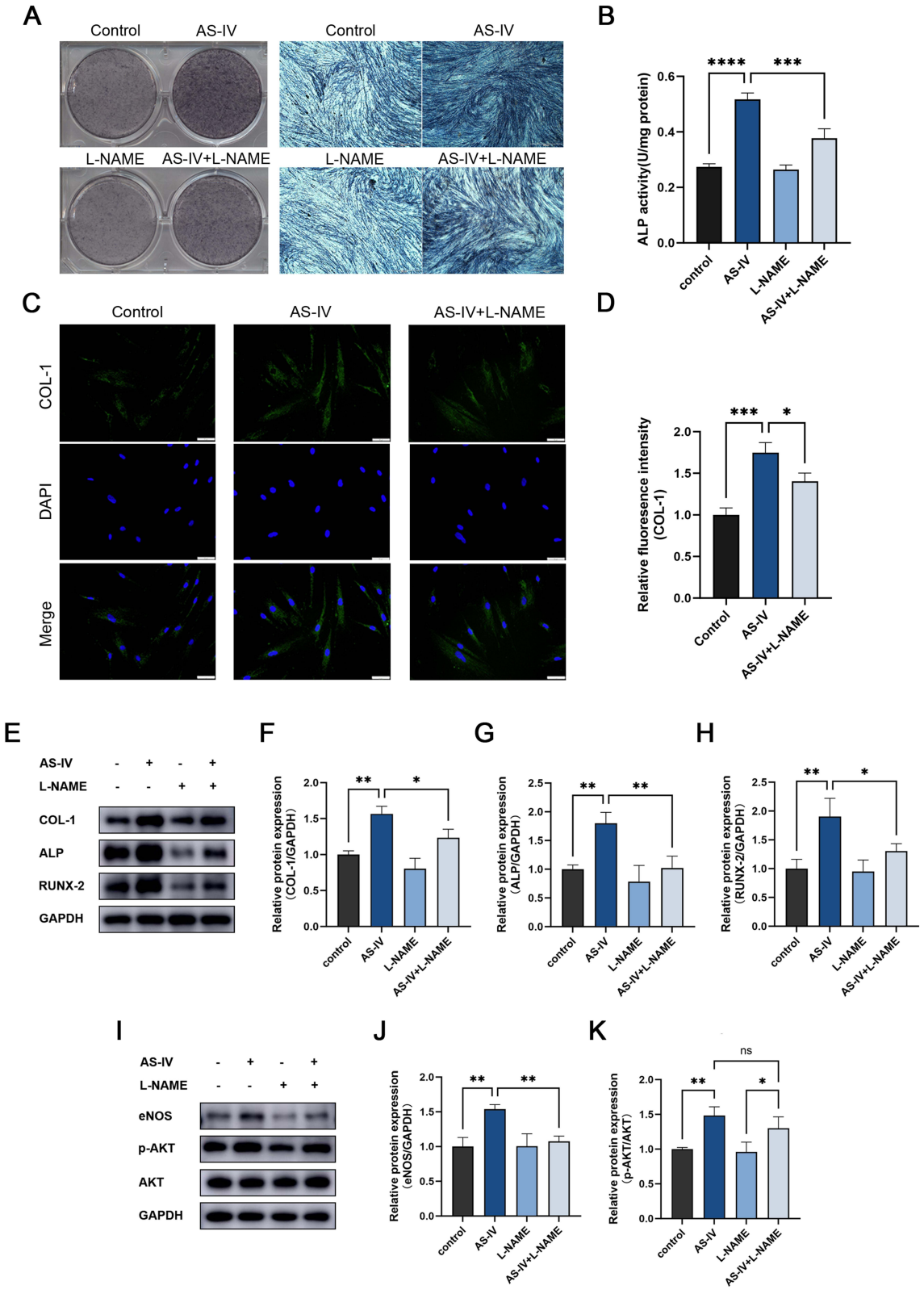

Figure 4 Effect of L-NAME on osteogenic differentiation and pathway-associated factor of PDLSCs following AS-IV incubation. (**A** and **B**) ALP staining(**A**) and ALP activity quantification(**B**) of PDLSCs affected by L-NAME. Scale bar: 500 μm. (**C** and **D**) Immunofluorescence staining(**C**) of COL-1 (green) and DAPI staining (blue) and quantification(D). Scale bar: 50 μm. (**E–H**) Western blot and semi-quantitative analysis of COL-1 (F), ALP(G), and RUNX-2 (**H**) in PDLSCs cultured with AS-IV and L-NAME. (**I–K**) Western blot and semi-quantitative analysis of eNOS(**J**) and p-AKT/AKT (**K**) in PDLSCs cultured with AS-IV and L-NAME. Data are presented as mean ± SD. **P*<0.05, ***P*<0.01, ****P*<0.001, *****P*<0.0001. ns: *P*>0.05. Each experiment was repeated five times.

https://doi.org/10.2147/DDDT.S514682

Contribution of PI3K/AKT Pathway Toward eNOS Activation

NO_2^- concentration assay revealed that AS-IV could promote NO secretion from PDLSCs, and this promotion effect was inhibited by LY294002 (Figure 3G). Immunofluorescence staining (Figure 3C and F) and Western blot (Figure 3P and Q) experiments indicated that LY294002 inhibited the activation of eNOS risen by AS-IV. Meanwhile, iNOS was not significantly affected by AS-IV and LY294002 (Figure 3L, N, P and R). Compared with the AS-IV group, the p-AKT/AKT concentration in the AS-IV+L-NAME group tended to decrease, but there was no statistically significant difference (Figure 4I and K).

Orthodontic Tooth Movement Distance and Alveolar Bone Evaluation

During the 14-day OTM (Figure 5A), all rats in the experiment survived and the devices were not dislodged. The OTM distance increased slightly in the AS-IV group, but there was no statistical difference (Figure 5B). BV/TV and Tb. Th in the tension-side alveolar bone were elevated in the AS-IV group, while on the pressure side, there was no statistical difference (Figure 5D and E). The result of Tb.Sp was no statistical difference (Figure 5F).

HE and IHC Staining Analysis

HE and IHC staining were conducted on the periodontal tension side. In the AS-IV group, the periodontal fibers were more dense and arranged more orderly, which were more irregular in the control group (Figure 6A). Lower expressions of ALP, COL-1 and eNOS were detected in the control group, and the AS-IV group showed the stronger signal (Figure 6B–D).

Discussion

PDLSCs have multi-directional differentiation potential, self-renewal ability, immunomodulatory ability, well histocompatibility, and abundant sources, which make them the most reliable and commonly used seed cells for periodontal tissue remodeling and regeneration.[40–43] Promoting PDLSCs osteogenic differentiation is essential for periodontal tissue engineering, which can be applied to several clinical areas, such as reconstruction of tissue defects, modulation of orthodontic tooth movement, and post-orthodontic retention. In this study, the tissue block approach was utilized to isolate and cultivate PDLSCs, and primary cells were verified by flow cytometry testing to be of mesenchymal origin and free of epithelial cell contamination. Osteogenic and lipogenic induction experiments demonstrated that the cultured PDLSCs had multidirectional differentiation potential.

Astragalus is a widely used Chinese herbal medicine, and Astragaloside IV is one of the main active ingredients for its efficacy. Previous researches have indicated that AS-IV can enhance the proliferation and osteogenic differentiation of other cells, thus exerting the effects of accelerating bone regeneration, repairing tibia defects, promoting osteogenic and angiogenic coupling, and ameliorating glucocorticoid-induced necrosis of the femoral head.[10–14,44] Therefore, we selected AS-IV and designed a series of related experiments to detect its effect on the osteogenic differentiation of PDLSCs. CCK-8 experiments showed that different concentrations of AS-IV in the experimental groups did not inhibit the proliferation of PDLSC. The ALP activity and alizarin red staining experiments indicated that AS-IV could promote PDLSC osteogenic differentiation, especially at the concentration of 20 μM. ALP is an essential osteoblast marker enzyme and its activity reflects the onset of the osteoblast calcification process.[45] RUNX-2 is a crucial factor in osteogenesis and can regulate related genes by binding to the core sites of promoters or enhancers.[46] COL-1 is the predominant and specific fibrillar collagen component of the bone matrix and is a necessary indicator of osteogenesis.[47] ALP, RUNX-2, and COL-1 were chosen as the target genes and proteins, and their changes were tested by qRT-PCR and Western blot. The results confirmed that AS-IV could stimulate the osteogenic differentiation of PDLSC, and 20 μM was selected as the optimum concentration for subsequent mechanism experiments.

PI3K/AKT is a common signaling pathway in bone metabolism. It is also involved in regulating PDLSCs osteogenic differentiation and activating classic osteogenic proteins including ALP, RUNX-2, and COL-1.[48,49] NO plays an essential regulatory role in bone homeostasis, and its increased expression promotes osteogenic differentiation of PDLSC and raises ALP activity in tension-side cells during orthodontic tooth movement.[22,23] The formation of endogenous NO

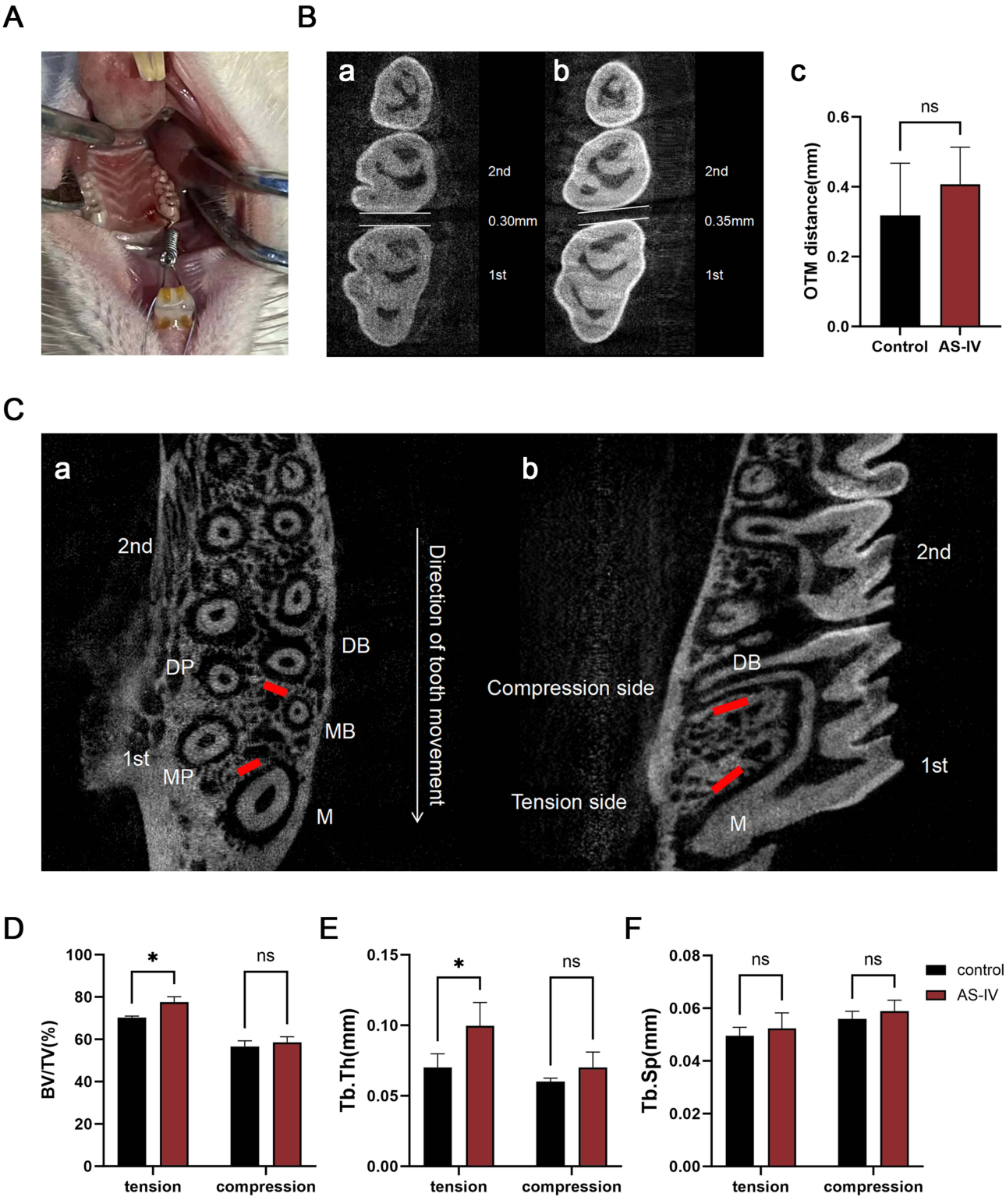

Figure 5 Model establishment, orthodontic tooth movement distance measure and evaluation of trabecular bone. (**A**) Intraoral photograph of orthodontic tooth movement model. (**B**) Orthodontic tooth movement distance (B-c) after intraperitoneal injections of physiological saline (B-a) and AS-IV (B-b) for 14 days. (**C**) Horizontal (C-a) and sagittal (C-b) sections of the molars and regions of interest. (**D–F**) Bone volume/total volume (BV/TV)(D), trabecular thickness (Tb.Th)(**E**) and trabecular separation (Tb.Sp) (**F**) of control group and AS-IV group. Data are presented as mean ± SD (n=8 rat/group). *P<0.05. ns: P>0.05.

Abbreviations: 1st, first molar; 2nd, second molar; M, mesial root; MB, mesiobuccal root; MP, mesiopalatal root; DB, distobuccal root; DP, distopalatal root.

https://doi.org/10.2147/DDDT.S514682

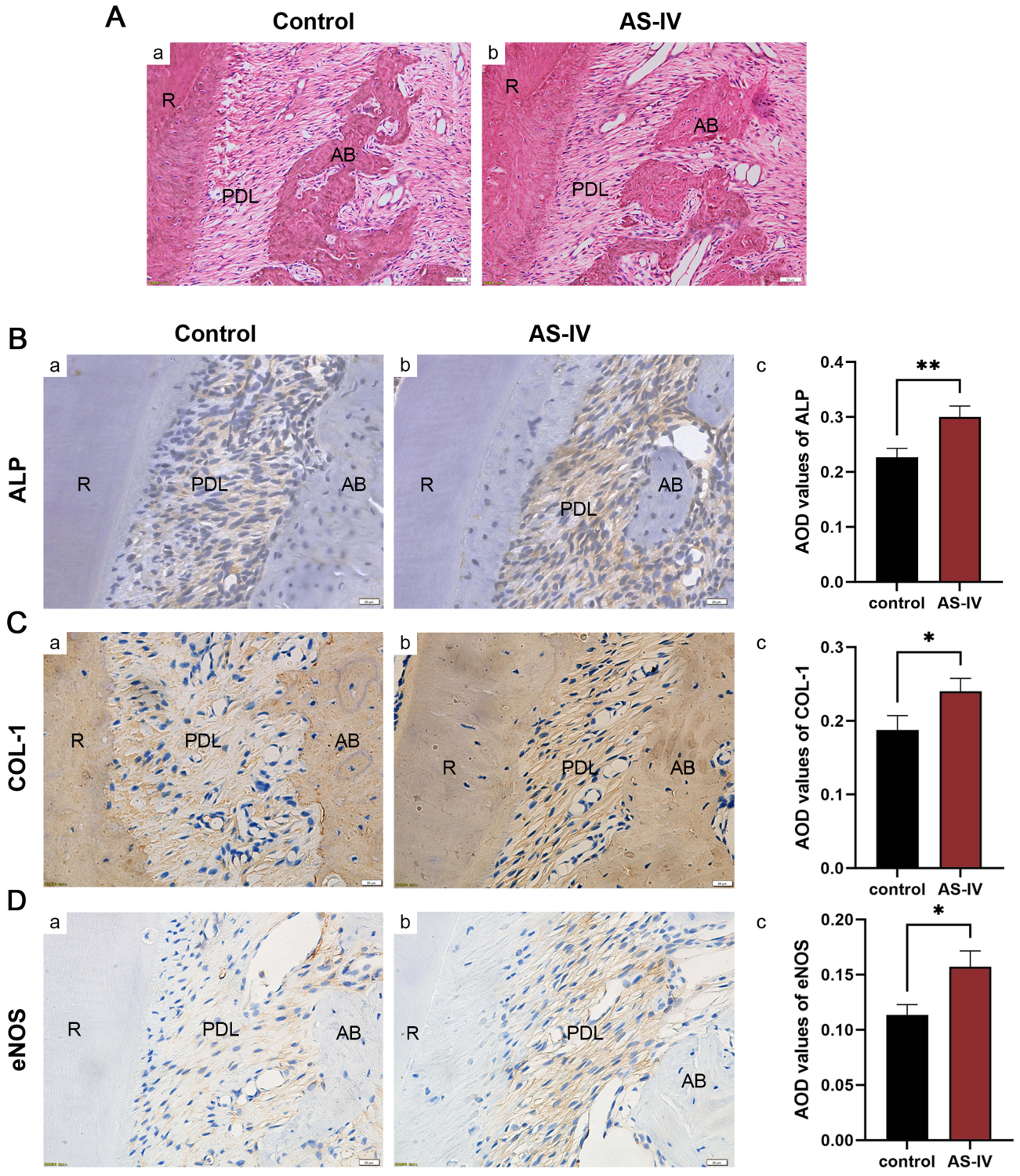

Figure 6 Hematoxylin and eosin staining and immunohistochemical staining. (**A**) HE staining of the tension-side periodontal tissues of the control group (A-a) and AS-IV group (A-b) after OTM for 14 days. Scale bar: 50 μm. (**B**) Expression of ALP of the control group (B-a) and AS-IV group (B-b) after OTM for 14 days and quantitative analysis (B-c). Scale bar: 20 μm. (**C**) Expression of COL-1 of the control group (C-a) and AS-IV group (C-b) after OTM for 14 days and quantitative analysis (C-c). Scale bar: 20 μm. (**D**) Expression of eNOS of the control group (D-a) and AS-IV group (D-b) after OTM for 14 days and quantitative analysis (D-c). Scale bar: 20 μm. Data are presented as mean ± SD (n=8 rat/group). **P*<0.05, ***P*<0.01.

Abbreviations: PDL, periodontal ligament; AB, alveolar bone; R, root.

depends on nitric oxide synthase, which mainly consists of eNOS, iNOS, and nNOS. Aguirre et al[24] found that the eNOS gene deletion inhibits ALP activity and calcium nodule production, and decreases bone volume and bone formation in mice. Afzal et al[50] demonstrated that eNOS defects can lead to decreased RUNX-2 expression and reduced bone mass and bone hardness in mice. Ehnes et al[51] found that inhibition of eNOS restrains calcification more than inhibition of iNOS at later stages of embryonic stem cell osteogenic culture. PI3K/AKT can also activate eNOS to promote osteogenesis. Ma et al's study[32] showed that glimepiride stimulates rat osteoblasts' osteogenic differentiation through the PI3K/AKT/eNOS pathway under the high-glucose conditions, and Zhai et al[33] discovered that icariin activates the PI3K-AKT-eNOS-NO-cGMP-PKG pathway to enhance the osteogenic development of rat bone marrow stromal cells. But there are few experiments that demonstrate the role of the PI3K/AKT/eNOS/NO pathway in the osteogenic process of human PDLSCs. Meanwhile, AS-IV has been proven to activate the PI3K/AKT/eNOS pathway through inducing PI3K and AKT phosphorylation.[15,35–37] Yang et al found that among the three nitric oxide synthases, PDLSCs expressed iNOS in addition to eNOS,[22] so we also investigated the effect of AS-IV on iNOS.

In the AS-IV group, the levels of ALP, RUNX-2, COL-1 and pathway proteins such as p-AKT/AKT and eNOS rose, and the NO production was elevated, while there was no significant difference in iNOS expression. These results suggest that AS-IV promotes osteogenesis, activates AKT and eNOS, and raises NO production mainly by activating eNOS but not iNOS. We added LY294002, an inhibitor of PI3K, and found that the p-AKT/AKT expression was significantly reduced, suggesting that LY294002 could indeed block the PI3K/AKT pathway. Compared with the AS-IV group, the levels of osteogenic proteins were significantly reduced in the AS-IV+LY294002 group, indicating that PI3K/AKT is a crucial pathway for the action of AS-IV. Next, we added the eNOS inhibitor L-NAME and found the lower osteogenic proteins' expression in the AS-IV+L-NAME group, proving that eNOS is also the action site. Meanwhile, the expression of eNOS and NO in the AS-IV+LY294002 group decreased, whereas iNOS did not significantly change, suggesting that PI3K/AKT affects NO production mainly by regulating eNOS rather than iNOS, which is consistent with the consequence of Zhai et al.[33] Although the addition of L-NAME led to a decrease in the p-AKT/AKT protein expression which AS-IV had increased, the result was not statistically different. The above results indicated an upstream-downstream relationship between the PI3K/AKT pathway and eNOS/NO during the action of AS-IV on PDLSCs. Some researchers found that cyclic tensile force stimulation promotes NO secretion and activates the PI3K/AKT pathway in PDLSCs, and the total NOS inhibitor attenuated the activation of PI3K/AKT.[23] This may be due to the existence of an intricate network of intracellular mechanisms that trigger different modulations in response to different external stimuli. It's worth noting that L-NAME did not completely inhibit osteogenic proteins activated by AS-IV, suggesting the probable involvement of additional signaling pathways beyond the PI3K/AKT/eNOS/NO axis. Existing studies have proved that AS-IV can activate multiple pro-osteogenic pathways in other cells, including AKT/GSK-3β/β-catenin, Wnt/β-catenin, STING/NF-κB, and MiR-124-3p.1/STAT3.[10–14,44] While our current study focused on elucidating the PI3K/AKT/eNOS/NO pathway in PDLSCs, these literature findings collectively suggest that AS-IV may exert its osteogenic effects through a complex network of complementary mechanisms. The relative contribution of each pathway likely depends on cellular context and microenvironmental factors, which warrants further systematic investigation in future studies.

Rats become sexually mature at the age of 6 weeks and possess active bone remodeling ability, compared with the humans at 11–12 years.[52] So we chose 6-week-old rats as in vivo subjects and established the orthodontic tooth movement model after 1 week of adaptive feeding and divided them into the control and AS-IV groups. Through scanning, 3D reconstruction, and measurement of the specimens, we found that the BV/TV and Tb. Th of tension-side alveolar bone were elevated by AS-IV. Meanwhile, it was found that the AS-IV group had a tendency to increase the tooth movement distance, which may be due to the biphasic effect of NO on osteoblastic and osteoclastic activities, thus potentially accelerating orthodontic tooth movement.[53] However, this difference was not statistically significant in this study. HE staining showed that the periodontal ligament cells of the AS-IV group were arranged more regularly. IHC staining demonstrated that the AS-IV group had a higher ALP and COL-1 expression level. These results indicated that AS-IV could promote periodontal osteogenesis on the tension side during OTM. The eNOS expression also increased in the experimental group, indicating that AS-IV promoted eNOS activation. Whereas, the overall expression level was slightly lower in both groups. Previous findings showed that eNOS was involved in periodontal tissue remodeling at an early stage, and the high local NO concentration produced negative feedback regulation after the lasting force application

to inhibit the overexpression of eNOS,[54,55] which is in accordance with our experimental results, and we will further explore this phenomenon in the subsequent experiments.

In conclusion, our study demonstrated for the first time that AS-IV promotes osteogenic differentiation of PDLSCs and identified the PI3K/AKT/eNOS/NO pathway as one of the signaling pathways involved in this process. These findings suggest AS-IV's potential as a natural therapeutic agent in periodontal and orthodontic applications, where its osteogenic properties could facilitate periodontal bone defect regeneration while simultaneously enhancing orthodontic treatment efficacy through bone remodeling promotion, improved anchorage control, and reduced post-treatment relapse.

The experimental design incorporates several key strengths, including the combined in vitro and in vivo methodology and the use of specific pathway inhibitors to establish causal relationships. Meanwhile, certain limitations must be acknowledged regarding the undetermined precise molecular targets of AS-IV (such as its PI3K interaction sites) and possible involvement of alternative signaling pathways (such as Wnt/β-catenin pathway). Furthermore, the current in vivo evidence derives solely from short-term rat studies, and there are differences in bone metabolism and pharmacokinetics between rats and humans. Therefore, caution is required when translating the findings from animal experiments to human applications. Further research will be conducted in the future to explore these aspects in more detail.

Conclusion

Our findings confirmed for the first time that AS-IV facilitates osteogenic differentiation of human PDLSCs, and verify the involvement of PI3K/AKT/eNOS/NO pathway in the process. Meanwhile, AS-IV promoted periodontal osteogenesis on the tension side during orthodontic tooth movement in rats. Our study could provide an experimental proof for the potential clinical application of AS-IV to promote periodontal tissue regeneration and mitigate relapse following OTM.

Abbreviations

AS-IV, Astragaloside IV; PDLSCs, periodontal ligament stem cells; CCK-8, cell counting kit-8; ALP, alkaline phosphatase; RUNX-2, runt-related transcription factor 2; COL-1, collagen I; PI3K/AKT, phosphatidylinositol 3 kinase/protein kinase B; NO, nitric oxide; NOS, nitric oxide synthase; eNOS, endothelial nitric oxide synthase; iNOS, inducible nitric oxide synthase; nNOS, neuronal nitric oxide synthase; OTM, orthodontic tooth movement; MEM, minimum essential medium; PBS, phosphate buffered saline; FBS, fetal bovine serum; qRT-PCR, quantitative real-time reverse transcriptase-polymerase chain reaction; DAPI, 2-(4-amidinophenyl)-6-indolecarbamidine dihydrochloride; L-NAME, Nω-Nitro -L-arginine methyl ester hydrochloride; micro-CT, micro-computer tomography; BV/TV, bone volume/total volume; Tb. Th, trabecular thickness; Tb.Sp, trabecular separation; HE, hematoxylin and eosin; IHC, immunohistochemical.

Data Sharing Statement

All data generated or analyzed during this study are included in this published article.

Ethics Approval and Consent to Participate

The study has been approved by the Ethics Committee of Shandong University School of Stomatology (No. 20221004, No. 20220343). The written informed consent was obtained from all patients from whom the teeth were extracted according to the protocol. Informed consent to participate was obtained from the parents or legal guardians of participant under the age of 18.

Funding

This work was supported by the Province Natural Science Foundation of Shandong Province, grant numbers ZR2021QH340.

Disclosure

The authors declare no competing interests.

References

1. Franzen TJ, Monjo M, Rubert M, Vandevska-Radunovic V. Expression of bone markers and micro-CT analysis of alveolar bone during orthodontic relapse. *Orthodontics Craniofacial Res*. 2014;17(4):249–258. doi:10.1111/ocr.12050
2. Iwayama T, Sakashita H, Takedachi M, Murakami S. Periodontal tissue stem cells and mesenchymal stem cells in the periodontal ligament. *Japan Dent Sci Rev*. 2022;58:172–178. doi:10.1016/j.jdsr.2022.04.001
3. Tomokiyo A, Wada N, Maeda H. Periodontal ligament stem cells: regenerative potency in periodontium. *Stem Cells Develop*. 2019;28 (15):974–985. doi:10.1089/scd.2019.0031
4. Aksel H, Zhu X, Gauthier P, Zhang W, Azim AA, Huang GTJ. A new direction in managing avulsed teeth: stem cell-based de novo PDL regeneration. *Stem Cell Res Ther*. 2022;13(1). doi:10.1186/s13287-022-02700-x
5. Zhao Z, Liu J, Weir MD, et al. Periodontal ligament stem cell-based bioactive constructs for bone tissue engineering. *Front Bioeng Biotechnol*. 2022;10. doi:10.3389/fbioe.2022.1071472
6. Sun C, Janjic Rankovic M, Folwaczny M, Otto S, Wichelhaus A, Baumert U. Effect of tension on human periodontal ligament cells: systematic review and network analysis. *Front Bioeng Biotechnol*. 2021;9. doi:10.3389/fbioe.2021.695053
7. Calabrese EJ. Human periodontal ligament stem cells and hormesis: enhancing cell renewal and cell differentiation. *Pharmacol Res*. 2021;173:105914. doi:10.1016/j.phrs.2021.105914
8. Hu N, Zhang X. Research progress on chemical constituents and pharmacological effects of astragalus membranaceus. *Information on TCM*. 2021;38(1):76–82.
9. Jiang W, Shili J, Ping L. Research progress on pharmacologic effects of astragaloside IV. *Chin Arch Tradit Chin Med*. 2019;37(9):2121–2124.
10. Wang F, Qian H, Kong L, et al. Accelerated bone regeneration by astragaloside IV through stimulating the coupling of osteogenesis and angiogenesis. *Int J Bio Sci*. 2021;17(7):1821–1836. doi:10.7150/ijbs.57681
11. Sun NY, Liu XL, Gao J, Wu XH, Dou B. Astragaloside-IV modulates NGF-induced osteoblast differentiation via the GSK3β/β-catenin signalling pathway. *Mol Med Rep*. 2021;23(1). doi:10.3892/mmr.2020.11657
12. Cao Y, Lv Q, Huang Z, Li Y. Astragaloside-IV induces the differentiation of bone marrow mesenchymal stem cells into osteoblasts through NMUR2-mediated Wnt/β-catenin pathway. *Regener Med*. 2023;18(6):471–485. doi:10.2217/rme-2022-0184
13. Shan H, Lin Y, Yin F, et al. Effects of astragaloside IV on glucocorticoid-induced avascular necrosis of the femoral head via regulating Akt-related pathways. *Cell Prolif*. 2023;56(11):e13485. doi:10.1111/cpr.13485
14. Li M, Niu Y, Tian L, et al. Astragaloside IV alleviates macrophage senescence and d-galactose-induced bone loss in mice through STING/NF-kappaB pathway. *Int Immunopharmacol*. 2024;129:111588. doi:10.1016/j.intimp.2024.111588
15. Lin X-P, Cui H-J, Yang AL, Luo J-K, Tang T. Astragaloside IV improves vasodilatation function by regulating the PI3K/Akt/eNOS signaling pathway in rat aorta endothelial cells. *J Vascu Res*. 2018;55(3):169–176. doi:10.1159/000489958
16. Ge B, S-l L, F-r L. Astragaloside-IV regulates endoplasmic reticulum stress-mediated neuronal apoptosis in a murine model of Parkinson's disease via the lincRNA-p21/CHOP pathway. *Exp. Mol. Pathol*. 2020;115:104478. doi:10.1016/j.yexmp.2020.104478
17. Gan L, Leng Y, Min J, Luo XM, Wang F, Zhao J. Kaempferol promotes the osteogenesis in rBMSCs via mediation of SOX2/miR-124-3p/PI3K/Akt/mTOR axis. *Eur J Pharmacol*. 2022;927:174954. doi:10.1016/j.ejphar.2022.174954
18. Miao S, Zhou J, Liu B, et al. A 3D bioprinted nano-laponite hydrogel construct promotes osteogenesis by activating PI3K/AKT signaling pathway. *Mater Today Bio*. 2022;16:100342. doi:10.1016/j.mtbio.2022.100342
19. Shim NY, Ryu JI, Heo JS. Osteoinductive function of fucoidan on periodontal ligament stem cells: role of PI3K/Akt and Wnt/beta-catenin signaling pathways. *Oral Dis*. 2022;28(6):1628–1639. doi:10.1111/odi.13829
20. Zhao X, Sun W, Guo B, Cui L. Circular RNA BIRC6 depletion promotes osteogenic differentiation of periodontal ligament stem cells via the miR-543/PTEN/PI3K/AKT/mTOR signaling pathway in the inflammatory microenvironment. *Stem Cell Res Ther*. 2022;13(1):417. doi:10.1186/s13287-022-03093-7
21. Yang S, Zhu B, Tian XY, et al. Exosomes derived from human umbilical cord mesenchymal stem cells enhance the osteoblastic differentiation of periodontal ligament stem cells under high glucose conditions through the PI3K/AKT signaling pathway. *Biomed Environ Sci*. 2022;35(9):811–820. doi:10.3967/bes2022.105
22. Yang S, Guo L, Su Y, et al. Nitric oxide balances osteoblast and adipocyte lineage differentiation via the JNK/MAPK signaling pathway in periodontal ligament stem cells. *Stem Cell Res Ther*. 2018;9(1):118. doi:10.1186/s13287-018-0869-2
23. Sun Y, Fu J, Lin F, et al. Force-induced nitric oxide promotes osteogenic activity during orthodontic tooth movement in mice. *Stem Cells Int*. 2022;2022:4775445. doi:10.1155/2022/4775445
24. Aguirre J, Buttery L, O'Shaughnessy M, et al. Endothelial nitric oxide synthase gene-deficient mice demonstrate marked retardation in postnatal bone formation, reduced bone volume, and defects in osteoblast maturation and activity. *Am J Pathol*. 2001;158(1):247–257. doi:10.1016/S0002-9440(10)63963-6
25. Armour K, Armour K, Gallagher M, et al. Defective bone formation and anabolic response to exogenous estrogen in mice with targeted disruption of endothelial nitric oxide synthase. *Endocrinology*. 2001;142(2):760–766. doi:10.1210/endo.142.2.7977
26. Meesters DM, Neubert S, Wijnands KAP, et al. Deficiency of inducible and endothelial nitric oxide synthase results in diminished bone formation and delayed union and nonunion development. *Bone*. 2016;83:111–118. doi:10.1016/j.bone.2015.11.006
27. Tan SD, Xie R, Klein-Nulend J, et al. Orthodontic force stimulates eNOS and iNOS in rat osteocytes. *J Dent Res*. 2009;88(3):255–260. doi:10.1177/0022034508330861
28. Nilforoushan D, Manolson MF. Expression of nitric oxide synthases in orthodontic tooth movement. *Angle Orthod*. 2009;79(3):502–508. doi:10.2319/050808-252.1
29. Alghanem AF, Abello J, Maurer JM, et al. The SWELL1-LRRC8 complex regulates endothelial AKT-eNOS signaling and vascular function. *Elife*. 2021;10. doi:10.7554/eLife.61313
30. Ning W, Li S, Yang W, et al. Blocking exosomal miRNA-153-3p derived from bone marrow mesenchymal stem cells ameliorates hypoxia-induced myocardial and microvascular damage by targeting the ANGPT1-mediated VEGF/PI3k/Akt/eNOS pathway. *Cell Signal*. 2021;77:109812. doi:10.1016/j.cellsig.2020.109812

31. Ji L, Su S, Xin M, et al. Luteolin ameliorates hypoxia-induced pulmonary hypertension via regulating HIF-2alpha-Arg-NO axis and PI3K-AKT-eNOS-NO signaling pathway. *Phytomedicine*. 2022;104:154329. doi:10.1016/j.phymed.2022.154329
32. Ma P, Gu B, Xiong W, et al. Glimepiride promotes osteogenic differentiation in rat osteoblasts via the PI3K/Akt/eNOS pathway in a high glucose microenvironment. *PLoS One*. 2014;9(11):e112243. doi:10.1371/journal.pone.0112243
33. Zhai YK, Guo XY, Ge BF, et al. Icariin stimulates the osteogenic differentiation of rat bone marrow stromal cells via activating the PI3K-AKT-eNOS-NO-cGMP-PKG. *Bone*. 2014;66:189–198. doi:10.1016/j.bone.2014.06.016
34. Lin RLC, Sung PH, Wu CT, et al. Decreased Ankyrin expression is associated with repressed eNOS signaling, cell proliferation, and osteogenic differentiation in osteonecrosis of the femoral head. *J Bone Joint Surg Am*. 2022;104(Suppl 2):2–12. doi:10.2106/JBJS.20.00465
35. Shi-yu Z, Yang S, Jing Z, et al. Effect of astragaloside IV on angiotensin II-induced inflammatory response of vascular endothelial cells and mechanism. *Chin J Chin Materia Medica*. 2022;47(21):5900–5907. doi:10.19540/j.cnki.cjcmm.20220725.701
36. Yu W, Hong Z, Yan-hao C, et al. To investigate the protective mechanisms of astragaloside IV on cardiac function in diabetic cardiomyopathy rats based on the PI3K/Akt/eNOS signaling pathway. *Lishizhen Med Materia Medica Res*. 2023;34(10):2329–2332.
37. Dongbo L, Wei L, Zaopeng H, et al. Effects of astragaloside IV regulating PI3K/AKT/eNOS signaling pathway on skin defects in diabetic rats. *J Tradit Chin Med Pharm*. 2022;28(7):20–26. doi:10.13862/j.cn43-1446/r.2022.07.004
38. Faraldi M, Mangiavini L, Conte C, et al. A novel methodological approach to simultaneously extract high-quality total RNA and proteins from cortical and trabecular bone. *Open Biol*. 2022;12(5):210387. doi:10.1098/rsob.210387
39. Arifin WN, Zahiruddin WM. Sample size calculation in animal studies using resource equation approach. *Malays J Med Sci*. 2017;24(5):101–105. doi:10.21315/mjms2017.24.5.11
40. Seo BM, Miura M, Gronthos S, et al. Investigation of multipotent postnatal stem cells from human periodontal ligament. *Lancet*. 2004;364 (9429):149–155. doi:10.1016/S0140-6736(04)16627-0
41. Ivanovski S, Gronthos S, Shi S, Bartold PM. Stem cells in the periodontal ligament. *Oral Dis*. 2006;12(4):358–363. doi:10.1111/j.1601-0825.2006.01253.x
42. Zhou LL, Liu W, Wu YM, Sun WL, Dorfer CE, Fawzy El-Sayed KM. Oral mesenchymal stem/progenitor cells: the immunomodulatory masters. *Stem Cells Int*. 2020;2020:1327405. doi:10.1155/2020/1327405
43. Li Q, Yang G, Li J, et al. Stem cell therapies for periodontal tissue regeneration: a network meta-analysis of preclinical studies. *Stem Cell Res Ther*. 2020;11(1):427. doi:10.1186/s13287-020-01938-7
44. Cao Y, Lv Q, Li Y. Astragaloside IV improves tibial defect in rats and promotes proliferation and osteogenic differentiation of hBMSCs through MiR-124-3p.1/STAT3 axis. *J Natural Prod*. 2021;84(2):287–297. doi:10.1021/acs.jnatprod.0c00975
45. Vimalraj S. Alkaline phosphatase: structure, expression and its function in bone mineralization. *Gene*. 2020;754:144855. doi:10.1016/j.gene.2020.144855
46. Narayanan A, Srinaath N, Rohini M, Selvamurugan N. Regulation of Runx2 by MicroRNAs in osteoblast differentiation. *Life Sci*. 2019;232:116676. doi:10.1016/j.lfs.2019.116676
47. Akhir HM, Teoh PL. Collagen type I promotes osteogenic differentiation of amniotic membrane-derived mesenchymal stromal cells in basal and induction media. *Biosci Rep*. 2020;40(12). doi:10.1042/BSR20201325
48. Han R, Dang R, Liu F, et al. Protein crotonylation promotes osteogenic differentiation of periodontal ligament stem cells via the PI3K-AKT pathway. *Stem Cells Feb*. 2024;23. doi:10.1093/stmcls/sxae018
49. Zhao B, Xiong Y, Zhang Y, Jia L, Zhang W, Xu X. Rutin promotes osteogenic differentiation of periodontal ligament stem cells through the GPR30-mediated PI3K/AKT/mTOR signaling pathway. *Exp. Biol. Med*. 2020;245(6):552–561. doi:10.1177/1535370220903463
50. Afzal F, Polak J, Buttery L. Endothelial nitric oxide synthase in the control of osteoblastic mineralizing activity and bone integrity. *J Pathol*. 2004;202(4):503–510. doi:10.1002/path.1536
51. Ehnes DD, Geransar RM, Rancourt DE, Zur Nieden NI. Exogenous nitric oxide enhances calcification in embryonic stem cell-derived osteogenic cultures. *Differentiation*. 2015;89(3–4):97–103. doi:10.1016/j.diff.2015.02.001
52. Xu B, Yang K. Changes in alveolar bone structure during orthodontic tooth movement in adolescent and adult rats: a microcomputed tomography study. *Orthod Craniofac Res*. 2023;26(4):568–575. doi:10.1111/ocr.12646
53. Yan T, Xie Y, He H, Fan W, Huang F. Role of nitric oxide in orthodontic tooth movement (Review). *IntJ Mol Med*. 2021;48(3). doi:10.3892/ijmm.2021.5001
54. Wei H, Hu L, Wen-jing C, Bin C, Chao M. Expression of eNOS in rat's orthodontic tooth movement. *Oral Biomedicine*. 2011;2(1):32–35.
55. Hui L, Jia L, Yang W, Minghe L. Effect of L-arginine on expression of eNOS in experimental tooth movement in rats Chinese Journal of Laboratory Diagnosis. 2019;23(7):1211–1216 doi:10.3969/j.issn.1007-4287.2019.07.038.